Journal of Hydrology xxx (xxxx) xxx

Contents lists available at ScienceDirect

Journal of Hydrology

journal homepage: www.elsevier.com/locate/jhydrol

Research paper

Intensification of extreme precipitation in arid Central Asia

Junqiang Yao [a,*], Yaning Chen [b,**], Jing Chen [a], Yong Zhao [c], Dilinuer Tuoliewubieke [a], Jiangang Li [a], Lianmei Yang [a], Weiyi Mao [a]

[a] Institute of Desert Meteorology, China Meteorological Administration, Urumqi 830002, China
[b] State Key Laboratory of Desert and Oasis Ecology, Xinjiang Institute of Ecology and Geography, Chinese Academy of Sciences, Urumqi, China
[c] School of Atmospheric Science, Chengdu University of Information Technology, Chengdu, China

ARTICLE INFO

This manuscript was handled by XXX, Editor-in-Chief, with the assistance of YYY, Associate Editor

Keywords:
Extreme precipitation
Central Asia
Precipitation

ABSTRACT

Changes in total and extreme precipitation are expected to intensify under climate warming. As Central Asia is among the driest regions in the world, more information is needed regarding the past and potential future changes in extreme precipitation in this region. In this study, we investigated changes in total and extreme precipitation in Central Asia based on observational records and Coupled Model Intercomparison Project 5 (CMIP5) model simulations. The results showed that all extreme precipitation-related indices except for consecutive dry days (CDD) experienced an increasing trend during 1936–2005. The annual total wet-day precipitation (PRCPTOT), daily intensity index (SDII), annual maximum 1- or 5-day precipitation amount (Rx1day and Rx5day), total annual number of days with precipitation exceeding heavy precipitation or very heavy precipitation thresholds (R10 and R20), and CDD were statistically robust. Generally, the statistically significant increasing trends are more pronounced in the wetter sub-regions, i.e. Northern and Southeastern Central Asia. Based on the CMIP5 model simulations, the PRCPTOT, Rx1day, and CDD in Central Asia are projected to increase robustly during 2006–2100 under representative concentration pathway (RCP) 4.5 and RCP 8.5; higher RCPs had higher rates of extreme precipitation and lower signal-to-noise ratios (SNRs). In addition, a considerable intensification of extreme precipitation and slight drought is predicted for the late 21st century (2071–2100). In Central Asia, the PRCPTOT, Rx1day, and CDD had an approximately linear relationship with global warming rates, with rates of 4.95%/K, 5.79%/K, and 2.79%/K, respectively, under RCP 4.5. The response rates were slightly lower under RCP 8.5 than under RCP 4.5 for these indices. The increase in total precipitation was mainly due to the intensification of extreme precipitation and a concomitant weakening of light precipitation, with a simultaneous overcompensation of increased evaporation due to global warming. Thus, our results suggest that total and extreme precipitation will intensify in Central Asia under a warming climate. Since increased extreme precipitation may lead to a heightened risk of flooding, water availability is predicted to remain limited over Central Asia.

1. Introduction

The latest Intergovernmental Panel on Climate Change (IPCC) report assessed global and regional changes in climatic extremes and concluded that global warming is aggravating the frequency, intensity, and duration of extreme climatic events (IPCC, 2013; Trenberth et al., 2015). For example, global daily extreme precipitation was projected to intensify under a warming climate; such as trend has been observed and is expected to continue (Alexander et al., 2006; Donat et al., 2013a; Sillmann et al., 2013; Donat et al., 2016, 2019). Changes in extreme precipitation have profound effects on the natural environment and human society and can seriously damage water resources, ecology, the environment, the biosphere, and socioeconomic systems (Sugiyama et al., 2010; IPCC, 2013; Zhang et al., 2017).

Generally, the spatial patterns of precipitation changes are heterogeneous, with different climatic regimes experiencing different changes. It is therefore important to investigate changes in total and extreme precipitation in different regions. Held and Soden (2006) suggested that

* Correspondence to: J. Yao, Institute of Desert Meteorology, China Meteorological Administration, No. 327, Jianguo Road, Urumqi 830002, China.
** Correspondence to: Y. Chen, State Key Laboratory of Desert and Oasis Ecology, Xinjiang Institute of Ecology and Geography, Chinese Academy of Sciences, Urumqi 830056, China.
E-mail addresses: yaojq@idm.cn (J. Yao), chenyn@ms.xjb.ac.cn (Y. Chen).

https://doi.org/10.1016/j.jhydrol.2020.125760
Received 9 August 2020; Received in revised form 6 November 2020; Accepted 9 November 2020
Available online 18 November 2020

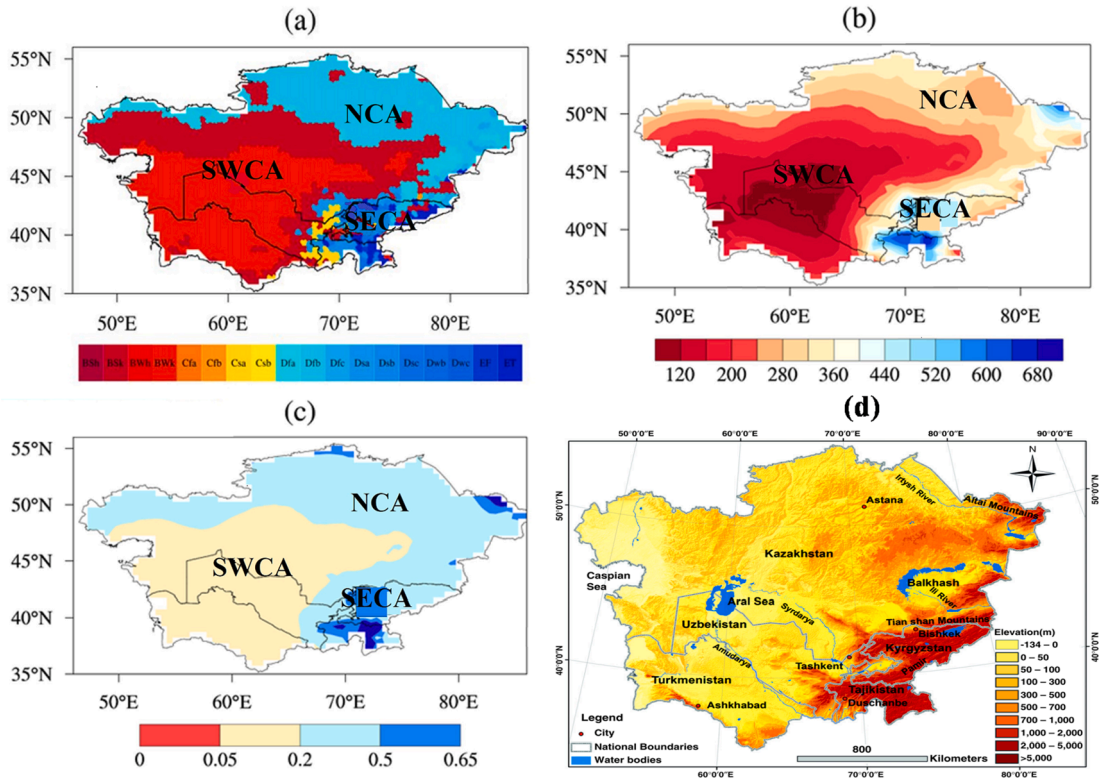

Fig. 1. The spatial distribution of (a) the Köppen climate classification, (b) average annual precipitation (mm/year), (c) aridity index (AI) values, and (d) topography in Central Asia.

wet regions will become wetter, while dry regions will become drier. Donat et al. (2016) reported significant increases in total and extreme precipitation in both the world's dry and wet regions throughout 1951–2010 based on both observations and climate-model simulations. Based on the most complete global daily-scale precipitation observations, both total and extreme precipitation have increased robustly over humid regions, but such robust changes have not been identified over water-limited regions (Donat et al., 2019). Twenty-first century climate projections have indicated increases in total precipitation over humid regions but no robust changes over arid regions. However, the intensification of extremes has been detected in both humid and arid regions worldwide (Donat et al., 2019). Thus, the intensification of extreme precipitation could lead to an aggravated worldwide risk of flooding, particularly in drier regions.

Central Asia is one of the driest regions in the world, and water resources scarcity directly affects ecosystems, economy, society, and sustainable development. Precipitation is the principal source of the water resources of the Central Asia regions, where is limited to wet season rainfall and winter snow. Thus, changes in total and extreme precipitation will have critical impacts on water resources and cryosphere and biosphere systems. Climate change in Central Asia has been extensively studied in recent decades. Central Asia experienced a rapid warming trend over the past century, and precipitation trends are highly variable, reflecting the high topographic and landscape diversity (Lioubimtseva et al., 2005; Lioubimtseva and Henebry, 2009; Chen et al., 2009). Precipitation records reflect an increasing trend in recent decades (Zhao and Zhang, 2016; Hu et al., 2016). Similar studies have documented that in arid regions of China, located in the eastern part of Central Asia, precipitation has displayed a significant increasing trend over the past 50 years, and changes in this area differ markedly from those in other areas, such as the Asia monsoon region (Shi et al., 2003; Li et al., 2016; Yao et al., 2016).

Central Asia's water cycle is especially sensitive and vulnerable to climate warming (UNDP, 2005; Parry et al., 2007; Lioubimtseva and Henebry, 2009; Hu et al., 2014; Zhao and Zhang, 2016), and some studies have indicated that Central Asia is likely to be strongly influenced by global warming (Chen et al., 2009; Hu et al., 2014; Zhao and Zhang, 2016). Global warming could accelerate the water cycle and alter the spatial-temporal distribution and intensity of precipitation, possibly resulting in increased extreme precipitation events (IPCC, 2013; Deng et al., 2014). Klein Tank et al. (2006) evaluated changes in extreme precipitation in Central and South Asia and identified a slightly anomalous change in extreme precipitation during 1961–2000. Zhang et al. (2017) investigated changes in extreme precipitation over Central Asia based on data from 22 meteorological stations and suggested that six investigated extreme precipitation indices displayed an increasing trend during 1938–2005. To predict future changes, Peng et al. (2019) evaluated the performances of Coupled Model Intercomparison Project 5 (CMIP5) models in simulating extreme precipitation over Central Asia and projected that extreme precipitation would increase robustly under representative concentration pathway (RCP) 8.5. However, a reduced intensity of extreme precipitation was projected under 0.5 °C less global warming in Central Asia (Peng et al., 2019).

Compared to the monsoon regions (East Asia and South Asia) and Mediterranean regions, less attention has been devoted toward arid regions in Central Asia. Despite the predicted changes in extreme events in Central Asia reported by some global-scale studies (O'Gorman and Schneider, 2009; Zhang et al., 2011; Shiu et al., 2012; Wartenburger et al., 2017; Donat et al., 2016, 2019; Du et al., 2019), information regarding past and projected changes in extreme events in Central Asia is still scarce. Previous analyses of climate change in Central Asia focused on extreme precipitation are rare in comparison to those focused on extreme temperature (Feng et al., 2017; Yu et al., 2020), and annual or seasonal precipitation (Hu et al., 2017; Chen et al., 2018; Luo et al., 2019; Jiang et al., 2020). To our knowledge, the extreme precipitation was no systematically analyzed due to the limited daily data resources resulting from the paucity of continuous instrumental stations and the relatively large errors in daily precipitation data measurements. Based

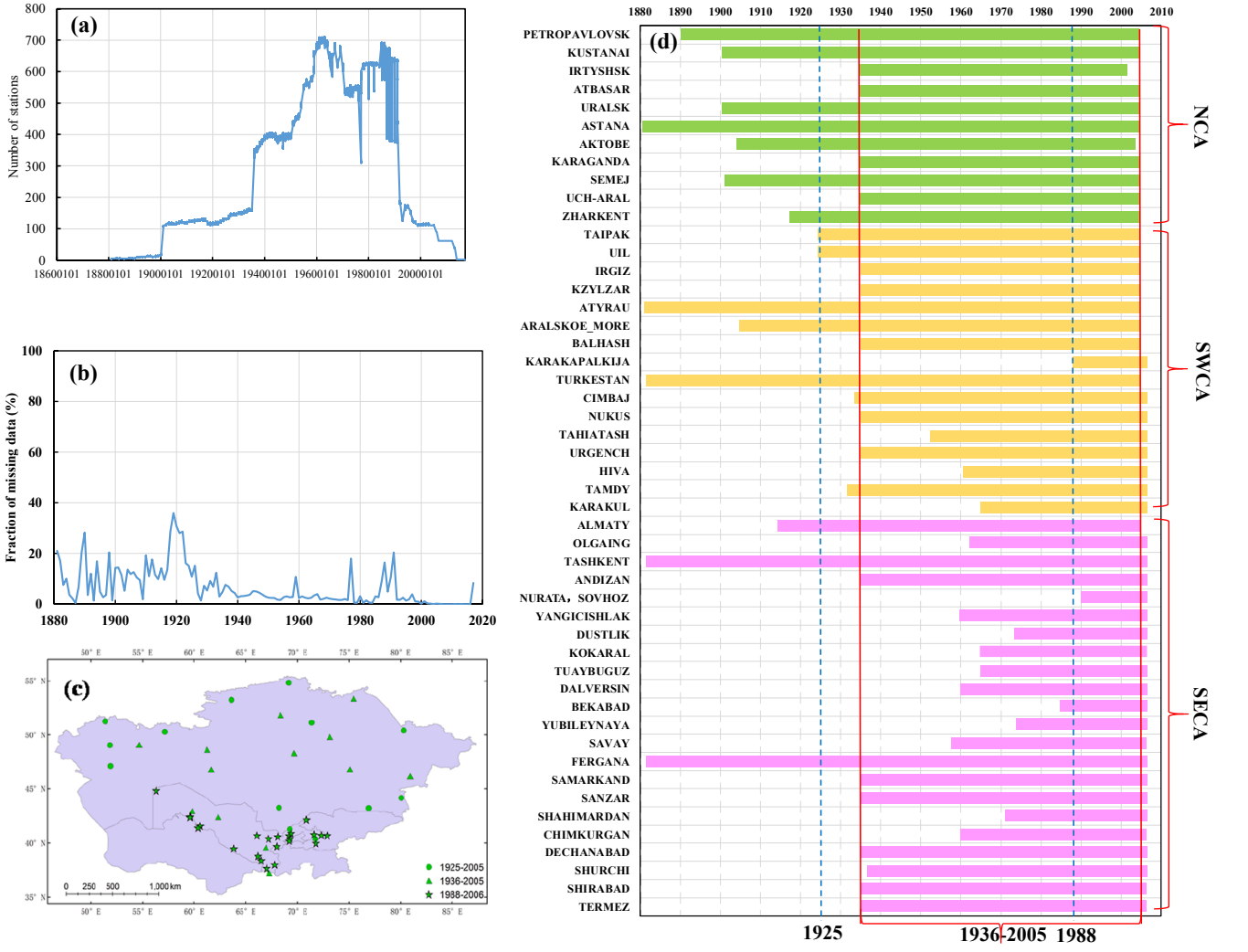

Fig. 2. (a) The total number of stations in Central Asia and (b) percentage of missing data in any given year, (c) station locations, and (d) the areal coverage for which continuous daily precipitation data were available from the meteorological stations used in this study. The green, orange, and pink rectangles represent the periods covered in the NCA, SWCA, and SECA regions, respectively. The dates in red brackets indicate years (1936–2005) where data were available from all of the stations used in the analysis. The blue dashed lines represent the years of 1925 and 1988, respectively. (For interpretation of the references to color in this figure legend, the reader is referred to the web version of this article.)

on daily observed precipitation data from over 500 land-based meteorological stations (with continuous instrumental data series in <50 stations) in Central Asia, this study aimed to investigate changes in total and extreme precipitation (using ten extreme indices) based on the observed daily precipitation records in Central Asia from 1936 to 2005. The projected change in total and extreme precipitation is analyzed using CMIP5 models simulations under the RCP4.5 and RCP8.5 scenarios. We also investigated the response of extreme events to global warming. This study has important implications for water resource management, natural hazard mitigation, and the provision of reliable future precipitation projections for arid Central Asia.

2. Data and method

2.1. Study area and sub-regions

2.1.1. Study area

Central Asia is located in the Eurasian hinterland and is one of the largest non-zonal arid regions in the world, far from any ocean. It has an area of about 402.8 × 10^4 km^2 and consists of five countries: Kazakhstan, Kyrgyzstan, Tajikistan, Turkmenistan, and Uzbekistan (Li et al., 2020). The physiographical landscape of Central Asia is characterized by a unique mountain-oasis-desert pattern (Chen et al., 2018). Its geomorphological features mainly include mountains, desert, basins, and valleys, including the Pamirs Plateau, Tianshan Mountains, Ural Mountains, Kyzylkum Desert, Karakum Desert, Fergana Valley, Turan Plain, and Kazakhstan Hills. The region has a typical temperate continental climate with low levels of precipitation that are determined by location and topography.

2.1.2. Sub-regions in Central Asia

Central Asia is one of the driest regions in the world, though its large geographical area contains complex climate regimes, various geomorphological landscapes, and different land covers and ecosystems. Based on climate classification, aridity index (AI, the ratio of annual precipitation to annual potential evapotranspiration, Liu et al., 2018), precipitation distribution, geomorphological landscapes, and land-cover conditions, Central Asia can be divided into three sub-regional areas: Northern Central Asia (NCA), Southwestern Central Asia (SWCA), and Southeastern Central Asia (SECA). The distribution of the sub-regional areas of Central Asia and their classification criteria are shown in Table S1 (in the Supporting information). Fig. 1 also showed the climate regimes, annual precipitation and AI in Central Asia.

The climate regime over the Central Asia is complex. Climate is

primarily influenced by the midlatitude westerly and stationary wave at the continental scales, and encompasses roughly three types of climate regimes when considering the contrast of the warm (May–October) and cold (November–April) seasonal precipitation (Dai and Wang, 2017). The first type is a westerlies climate and precipitation is concentrated in the warm season in the NCA region. The second is Mediterranean-like climate (MDC-like) with relatively uniform seasonal precipitation distribution, which exists mostly in the SWCA region. The last type is an MDC-like and Plateau climate, including the western Tianshan Mountain and Pamir Plateau (SECA region) with precipitation concentrated in the cold season. Previous studies have also shown that the teleconnection and large-scale ocean–atmospheric patterns are responsible for the precipitation variations in Central Asia, including Silk Road pattern, El Niño Southern Oscillation (ENSO), Indian Ocean Basin Mode (IOBM), and Arctic Oscillation (AO) (Chen and Huang, 2012; Huang et al., 2015; Lu et al., 2019; Yao and Chen, 2015; Guan et al., 2019; Yao et al., 2020).

2.2. Observations

Daily observed precipitation data from a total of 568 land-based meteorological stations covering the five Central Asian countries were obtained from the Global Historical Climatology Network-Daily Database (GHCN-D) and Global Telecommunications System (GTS). These data are available from the National Climatic Data Center (NCDC) of the National Oceanic and Atmospheric Administration (NOAA) (ftp://ftp.ncdc.noaa.gov/pub/data/gsod) (Menne et al., 2012).

High quality observation data are a prerequisite for calculating and analyzing climate extremes at a regional level (Alexander, 2016; Zhang et al., 2017). However, the observation series of precipitation are prone to inhomogeneous biases depending on the condition of gauging stations, anthropogenic impacts, observational accuracy, observational devices, and so on. Thus, these data series were submitted to quality control and homogeneity tests using RClimDex and RHtest software, respectively. This software is freely available from the Expert Team on Climate Change Detection and Indices (ETCCDI) website (https://www.wcrp-climate.org/etccdi). It is difficult to obtain spatially homogeneous station precipitation records throughout the Central Asian countries. Long-term continuous data were limited due to the absence of meteorological data for Central Asia during the 1990s and after the fall of the former Soviet Union. To be included in the analysis, the daily data series required a homogeneous period of at least 20 years, ending no earlier than 2005 and featuring data gaps of <10%. As a result, 49 high-quality meteorological stations with long-term daily precipitation data were identified for use in the study, and 32 stations were used to study precipitation variability over a 70-year period (January 1, 1936 to December 31, 2005), while only 15 stations were used to study changes an 81-year period (January 1, 1925 to December 31, 2005). As many stations as possible were selected based on the length, completeness, homogeneity, representativeness, and coverage of their time series data. Data gaps were supplemented using median precipitation data from at least three neighboring stations (Gemmer et al., 2011).

Fig. 2 shows the total number of stations in Central Asia, their location, the proportion of missing data from records in any given year, and the period for which continuous data were available from each station. A continuous daily data time series was obtained from only two countries in Central Asia, Kazakhstan (21 stations) and Uzbekistan (28 stations); extensive mountainous topography and deserts in other countries restricted data collection. Many stations were missing data prior to 1925 and in the 1990s, with periods of missing data accounting for >10% of the total data record. Eleven, 16, and 22 stations were selected from the NCA, SWCA, and SECA regions, respectively. In addition, the annual total precipitation of the selected stations has a notable spatial homogeneity in different Köppen climate zones in Central Asia.

Table 1
The extreme precipitation indices used in this study.

Index	Indicator name	Definition	Units
Intensity indices			
PRCPTOT	Annual total wet-day precipitation	Annual total precipitation from days ≥1 mm	mm
SDII	Simple daily intensity index	The ratio of annual total precipitation to the number of wet days (≥1 mm)	mm/day
Rx1day	Max 1-day precipitation amount	Annual maximum 1-day precipitation	mm/day
Rx5day	Max 5-day precipitation amount	Annual maximum consecutive 5-day precipitation	mm
Percentile-based threshold indices			
R95pTOT	Contribution from very wet days	100 × R95p/PRCPTOT (annual total precipitation from days > 95th percentile)	%
R99pTOT	Contribution from extremely wet days	100 × R99p/PRCPTOT (Annual total precipitation from days > 95th percentile)	%
Frequency indices			
R10	Number of heavy precipitation days	Annual days with precipitation ≥10 mm	days
R20	Number of very heavy precipitation days	Annual days with precipitation ≥20 mm	days
Duration indices			
CDD	Consecutive dry days	Maximum number of consecutive days when precipitation <1 mm	days
CWD	Consecutive wet days	Maximum number of consecutive days when precipitation ≥1 mm	days

2.3. CMIP5 model simulations

The outputs of historical runs and future projections from 20 CMIP5 models (ACCESS1-0, bcc-csm1-1, CanESM2, CMCC-CM, CMCC-CMS, CNRM-CM5, CSIRO-Mk3-6-0, GFDL-ESM2G, GFDL-ESM2 M, HadGEM2-CC, HadGEM2-ES, inmcm4, IPSL-CM5A-LR, IPSL-CM5B-LR, MIROC5, MIROC-ESM-CHEM, MPI-ESM-LR, MPI-ESM-MR, MRI-CGCM3, NorESM1-M) (Supplementary Table S2)were used in this analysis. All of the models focused on the two future Representative Concentration Pathways (RCP 4.5 and RCP 8.5), which represent moderate and high radiative-forcing scenarios to simulate possible future changes in total and extreme precipitation (Donat et al., 2016). For each run, we merge the corresponding historical (1936–2005) and future scenario (2006–2100) simulations to give transient time series from 1936 to 2100 for both the historical plus RCP4.5 scenario and historical plus RCP8.5 scenario simulations (Donat et al., 2016; Donat et al., 2019). The first ensemble member (the first realization, initialization, and set of perturbed physics, which is denoted "r1i1p1") simulation was used for all models. The CMIP5 multi-model ensemble (CMIP5 MME) mean was defined as the equally weighted mean of all model runs (Herger et al., 2018; Peng et al., 2019).

According to the IPCC Fifth Assessment Report (AR5), the baseline period of 1986–2005 in historical simulations is referred to as the 'present-day' (Stocker et al., 2013; Zhang et al., 2018). And the periods of 2021–2050 and 2071–2100 under RCP4.5 and RCP8.5 represent the middle and late of the 21st century, respectively. The changes of the warming scenarios are compared to the present-day conditions.

2.4. Definitions of extreme precipitation indices

The extreme indices developed and recommended by the ETCCDI to investigate extreme climatic variations are 10 extreme precipitation-based indices (Frich et al., 2002; Peterson and Manton, 2008; Zhang et al., 2011). Most of the indices were developed to measure 'moderate extremes' in a sense that were typically occurring at least once a year (Zhang et al., 2011). Generally, extreme precipitation indices can be classified into one of four categories: Intensity indices, Percentile-based

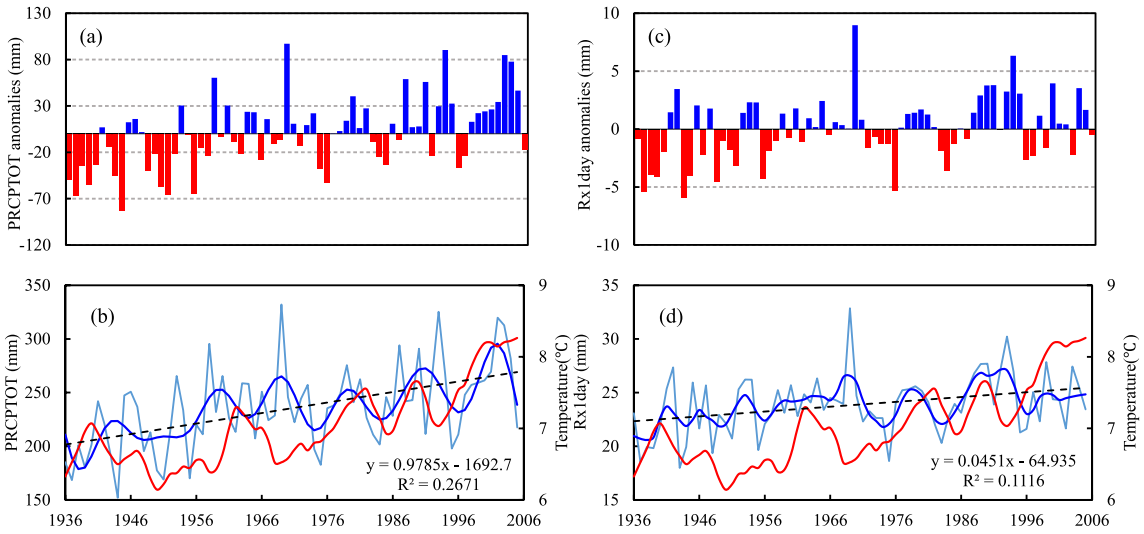

Fig. 3. Regionally averaged PRCPTOT (a) and Rx1day (b) anomalies in Central Asia, 1936–2005, based on the mean precipitation from 1936 to 2005; Changes in regional PRCPTOT (c) and Rx1day (d) in Central Asia from 1936 to 2005 (light blue line), with a trend line (black dotted line) and lowpass filtering (blue solid curve). The red solid curve represents the lowpass filtering of the air temperature in Central Asia. (For interpretation of the references to color in this figure legend, the reader is referred to the web version of this article.)

threshold indices, Frequency indices, and Duration indices.

Table 1 lists the definitions (or detailed calculation method) and units of ten ETCCDI indices (Alexander et al., 2019). All the indices have been calculated as annual values based on the daily time series. Each of the 10 ETCCDI extreme precipitation index values was calculated by applying the RclimDex procedure to the daily precipitation data of homogenized series of in situ-observations and CMIP5 model outputs. The thresholds were determined using wet-day data for 1936–2005. Annual index values were calculated if no >15 days were missing in a year (McGree et al., 2019).

2.5. Trend calculation and regional averaging

Linear trends of the extreme indices in the observational data and CMIP5 ensemble mean were estimated using the non-parametric Sen's slope estimator (Sen, 1968), and trend significance was statistically determined using the Mann-Kendall test (MK test) (Mann, 1945; Kendall, 1975). Sen's slope estimator is a non-parametric method that can be used to estimate the slope of linear trends in extreme index time series (Aguilar et al., 2005; Zhang et al., 2005; Yao et al., 2018). The MK test is a widely used method for the detection of non-parametric trends and

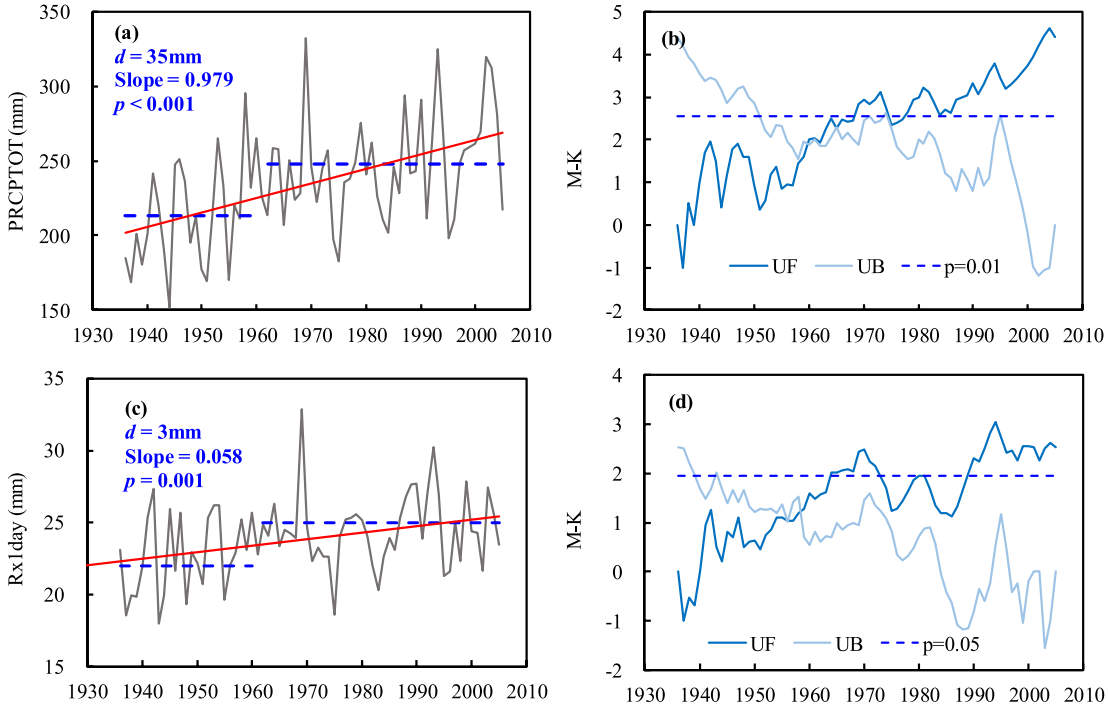

Fig. 4. Time series trend and Mann-Kendall test for abrupt changes of PRCPTOT (a, b) and Rx1day (c, d) for Central Asia from observations. Gray lines: annual precipitation time series; red lines: linear trend Sen-slope estimate; blue dashed lines: average values for 1936–1960 and 1961–2005; *d* value: the difference between the averages for the two time periods; *slope*: linear trend estimated via Sen's slope (unit: mm per year); and *p*-value: the trend significance from the Mann-Kendall test. The UF represents the statistical series of the standard normal distribution, and the UB represents the reverse statistical series. (For interpretation of the references to color in this figure legend, the reader is referred to the web version of this article.)

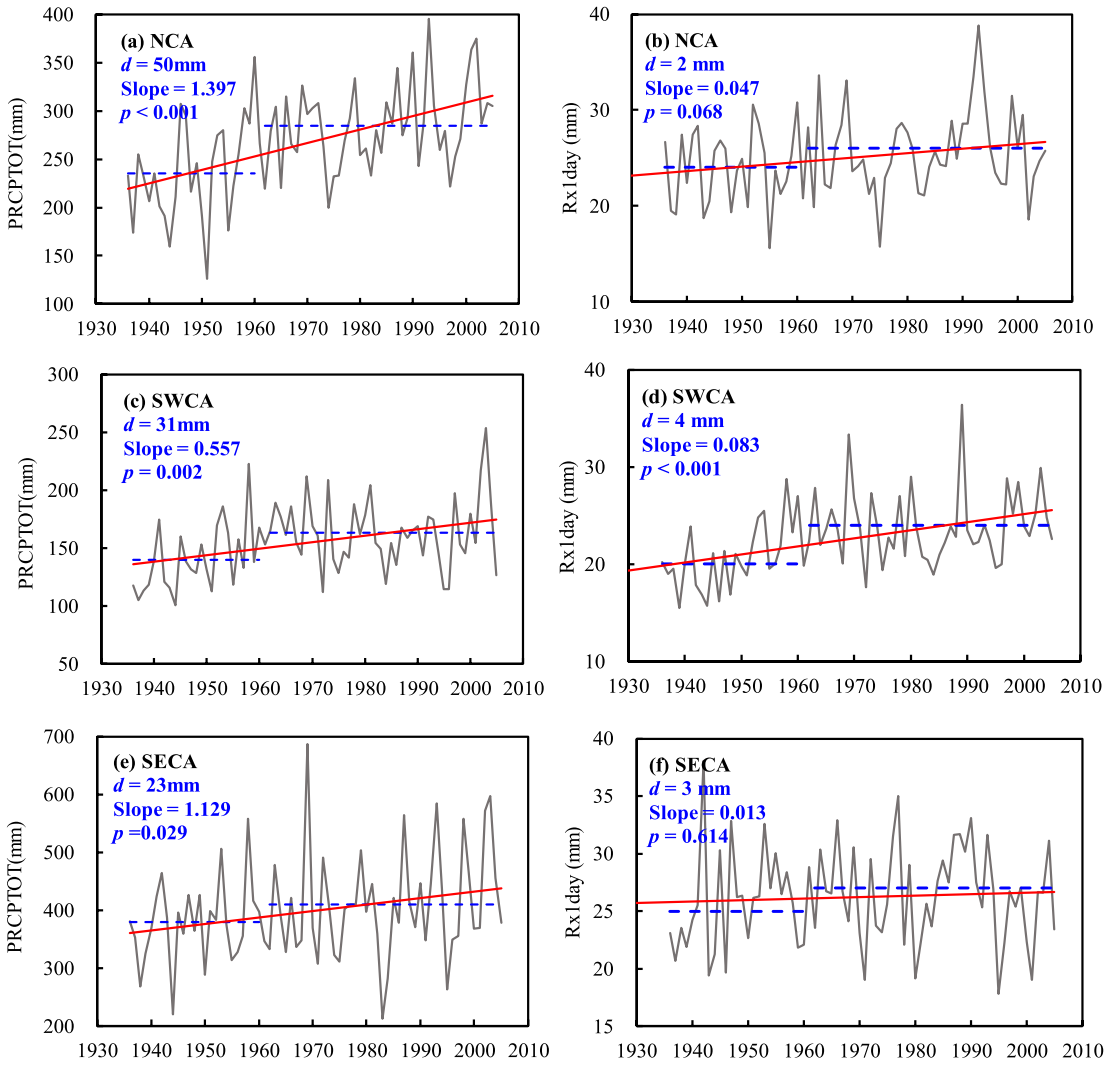

Fig. 5. Changes in PRCPTOT and Rx1day in Central Asian sub-regions based on observations. Gray lines: PRCPTOT (left column) and R1xday (right column); red lines: linear trend estimated via Sen's slope; blue dashed lines: average values for 1936–1960 and 1961–2005; *d* value: the difference between the averages for the two time periods; *slope*: linear trend estimated via Sen's slope (unit: mm per year); and *p*-value: trend significance based on a Mann-Kendall test. (For interpretation of the references to color in this figure legend, the reader is referred to the web version of this article.)

abrupt changes in data series (Wang et al., 2013; Yao et al., 2016, 2018).

Regional averages of the indices were produced by combining all available station index values in the regions studied. For most stations, where data series had a common start and end time and were relatively complete, the arithmetic mean method was used. These stations were distributed over an expansive geographical area and in different environments; thus, precipitation analyses were processed on a sub-regional basis. The stations were divided within the three sub-regions (NCA, SWCA, and SECA) as shown in Fig. 1, and regional trends in extreme precipitation were calculated based on regional arithmetic average data series from 11, 12, and 9 stations in the NCA, SWCA, and SECA regions, respectively, for 1936–2005.

Observed data from 32 (49) stations were used to investigate changes in extreme precipitation for 1936–2005 (1985–2005), and 15 stations were selected for the longer period of 1925–2005. To further understand changes in extreme precipitation in different periods, the period of 1936–2005 was divided into two phases, 1936–1960 and 1961–2005, and probability distribution functions (PDFs) were computed for the extreme indices in both phases. For the CMIP5 models, PDFs were calculated for the historical simulations (1936–1960 and 1961–2005) and 21st century projections (2021–2050 and 2071–2100). The PDF is the integral of the probability density function, which is provided the probability of an event that will occur in a given interval (Kay, 2012).

2.6. Response of extreme precipitation change to global warming

To derive the response of extreme precipitation to global warming, we investigated the future projected precipitation changes as a function of global mean surface air temperature increases. The extreme precipitation differences (2071–2100 relative to 1985–2005) are plotted against the global mean near-surface air temperature differences. The linear regression between them is derived as the response rate for each model, separately.

The signal-to-noise ratio (SNR) was defined as the ratio of the MME median to inter-model standard deviation (Pendergrass et al., 2015). An SNR > 1.0 implies robust changes compared to the model uncertainty. All calculations are conducted on native grids in the models.

3. Results

3.1. Observed changes in extreme precipitation

3.1.1. Changes in total annual precipitation

Changes in PRCPTOT and Rx1day were experienced in Central Asia

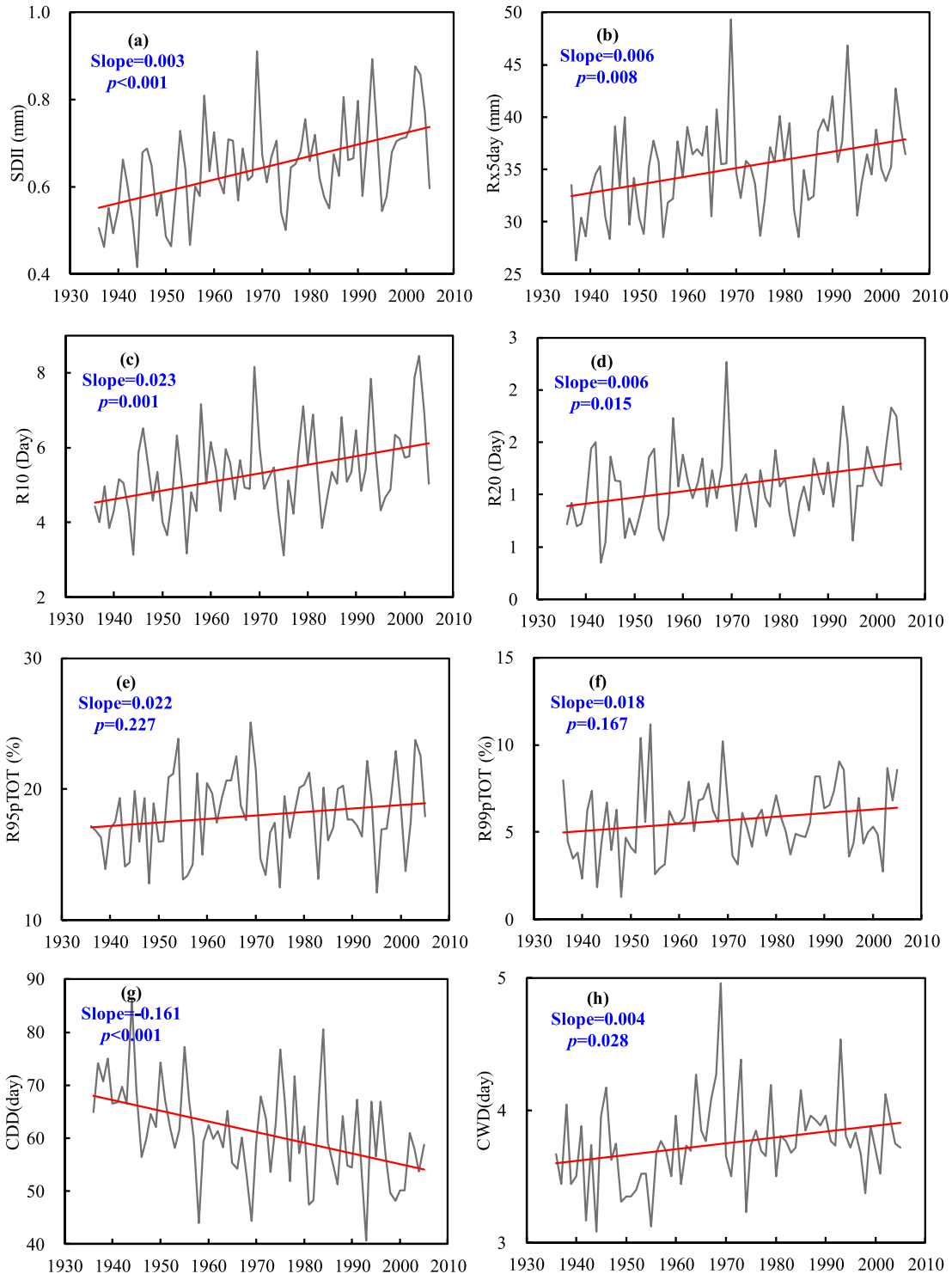

Fig. 6. As in Fig. 4, but for precipitation spell indices. The units are mm per year (a and b), day per year (c, d, g and h), and % per year (e and f), respectively.

during 1936–2005 (Fig. 3). The driest periods occurred in 1936–1957, while the wettest periods occurred in 1997–2004. Precipitation amounts in 1969 (approximately 332.1 mm) and 1944 (approximately 152.0 mm) represented the wettest and driest years on record, respectively (Fig. 3b). Fig. 3b shows the time series of regionally averaged PRCPTOT in Central Asia, indicating a fluctuating record that increased over the period of 1936–2005, especially from the 1960s. The time series of regionally averaged Rx1day was generally consistent with the PRCPTOT in Central Asia (Fig. 3c and d).

Annual mean temperature in Central Asia has increased at an average rate of 0.22 °C/decade during 1936–2005 based on the CRU dataset. This rate is even higher for the period from 1960s to the 2000s, at about 0.30 °C/decade. Extreme precipitation is expected to intensify with climate warming. Fig. 3c and d shows the relationship between PRCPTOT and Rx1day, and surface air temperature in Central Asia. The results indicate that the PRCPTOT and Rx1day are significantly positively correlated with the temperature, especially from the 1960s (the correlation coefficient is 0.62 and 0.37, respectively, $p < 0.05$). Thus, the changes in precipitation totals and extremes are among the most relevant consequences of climate warming.

Table 2
Regional and sub-regional trends in precipitation extreme indices.

	CA			NCA			SWCA			SECA		
	1925–2005	1936–2005	1988–2005	1925–2005	1936–2005	1988–2005	1925–2005	1936–2005	1988–2005	1925–2005	1936–2005	1988–2005
PRCPTOT (mm/decade)	9.86**	9.78**	19.61	12.28**	13.97**	10.37	4.47*	5.57**	8.52	10.87**	3.59	24.94
SDII ([mm/day]/decade)	0.027**	0.027**	0.054	0.034**	0.039**	0.025	0.012*	0.015**	0.038	0.030**	0.020	0.068
Rx1day (mm/decade)	0.58**	0.45**	−0.39	0.57*	0.47	−2.96	1.17**	0.83**	0.13	0.19	0.13	−1.17
Rx5day (mm/decade)	0.66**	0.79**	0.39	0.84*	1.19**	−4.24	0.21	0.46	0.90	0.96*	0.69	0.54
R95pTOT (%/decade)	0.22	0.27	2.41	0.15	0.42	0.55	0.34	0.24	2.25	0.39	0.13	4.37
R99pTOT (%/decade)	0.18	0.21	0.41	0.19	0.19	−1.46	0.32	0.43*	1.71	0.01	0.07	−0.98
R10 (day/decade)	0.23**	0.23**	1.23	0.20**	0.29**	0.53	0.12	0.12*	0.79	0.46**	0.32*	1.80
R20 (day/decade)	0.06*	0.06**	0.47	0.04	0.04	−0.11	0.04	0.04*	0.24	0.14*	0.11	0.86
CDD (day/decade)	−1.61**	−2.02**	−2.45	−1.72**	−1.79**	−4.33	−1.72*	−2.38**	1.05	−1.21	−3.23*	−6.46
CWD (day/decade)	0.04	0.04*	−0.09	0.06	0.07	−0.12	0.00	0.02	−0.04	0.04*	−0.02	−0.14

** Trends significant at the 99% significance level.
* Trends significant at the 95% significance level.

Observations showed statistically significant ($p \leq 0.001$) increases in both the PRCPTOT and Rx1day indices in Central Asia with average change rates of 9.79 mm and 0.58 mm/day per decade, thus indicating a continuous regional increase in both precipitation indices over the 70-year period (Fig. 4a and c). The MK test indicated that both the PRCPTOT and Rx1day indices sharply increased, with an abrupt change in 1960 at the 99% (95%) significance level (Fig. 4b and d). Based on the identified abrupt change, the study period was divided into two periods: 1936–1960 and 1961–2005, with both indices markedly increasing after 1960. The difference between the averages of the two periods was 35 mm and 3 mm/day for the PRCPTOT and Rx1day indices, respectively (Fig. 4a and c).

Fig. 5 shows the change in PRCPTOT and Rx1day values for sub-regions in Central Asia from 1936 to 2005. Regarding the PRCPTOT indices, the NCA region had an increasing trend of 13.97 mm per decade ($p < 0.001$), followed by SECA with a rate of increase of 11.29 mm per decade ($p = 0.029$) and SWCA with a rate of increase of 5.57 mm per decade ($p = 0.002$). Among the sub-regions, the differences between the averages of the two periods of 1936–1960 and 1961–2005, were 50, 23, and 31 mm (for NCA, SWCA, and SECA, respectively) (Fig. 5a, c, and e). For the Rx1day indices, the SWCA region had the highest rate of increase of 0.83 mm/day per decade ($p < 0.001$), followed by NCA with a rate of 0.47 mm/day per decade ($p = 0.068$) and SECA with a rate of 0.13 mm/day per decade ($p = 0.614$). The differences between the averages of the two periods were 4, 2, and 3 mm/day in NCA, SWCA, and SECA, respectively (Fig. 5b, d, and f).

Regarding the regionally averaged trends over the 70-year period, some of the extreme precipitation indices, including SDII, Rx5day, R10, R20, R95pTOT, R99pTOT, and CWD, presented increasing trends; CDD presented a decreasing trend. Moreover, most of these indices (SDII, Rx5day, R10, R20, and CDD) had statistically significant trends at the 95% significance level (Fig. 6).

Table 2 presents the regional and sub-regional trends for the extreme precipitation indices in Central Asia during the different periods. Generally, the statistically significant increasing trends are generally more pronounced in the wetter sub-regions, i.e. NCA and SECA. The sub-regional time series of SDII in Central Asia was consistent with the observed increase in PRCPTOT indices. For the Rx5day indices, the NCA region had the highest rate of increase of 1.19 mm per decade ($p < 0.001$), and SECA region has a positive trend of 0.96 mm per decade which is significant for the period 1925–2005. The observed R95pTOT and R99pTOT trends increased in all sub-regions, but only the SWCA trend was statistically significant for 1936–2005. The R10 and R20 indices displayed positive trends, with the highest rate of increase in the SECA region for 1936–2005. The R10 trend was statistically significant in all sub-regions, and in SECA sub-region (0.14 day per decade) for the period 1925–2005. The CDD indices decreased over the 70-year period, and all sub-regions displayed negative trends for the 1936–2005 period. In contrast, a significant increase was identified in the CWD values. In addition, most extreme precipitation indices had statistically significant trends ($p < 0.05$) over 1925–2005 in Central Asia, except for the R95pTOT, R99pTOT, and CWD. Most of the indices had larger trends over the 1988–2005 than other periods, but no statistically significant trends for all indices were found during 1988–2005. It is possible related to the shorter period.

3.1.2. Probability distribution functions

Fig. 7 shows the PDFs for all extreme precipitation indices and indicates the differences in precipitation characteristics between the two periods: 1936–1960 (red curve) and 1961–2005 (blue curve). Fig. 7 also shows a remarkable rise and shift toward the right of the peak distribution with time, indicating that the frequency and intensity of extreme precipitation events increased in the most recent period, except for the R99pTOT and CDD indices. For these indices, the CDD has a noticeable drop and shift toward the left of the peak location in the second period, while the PDF peak value is shifted toward the right and its value

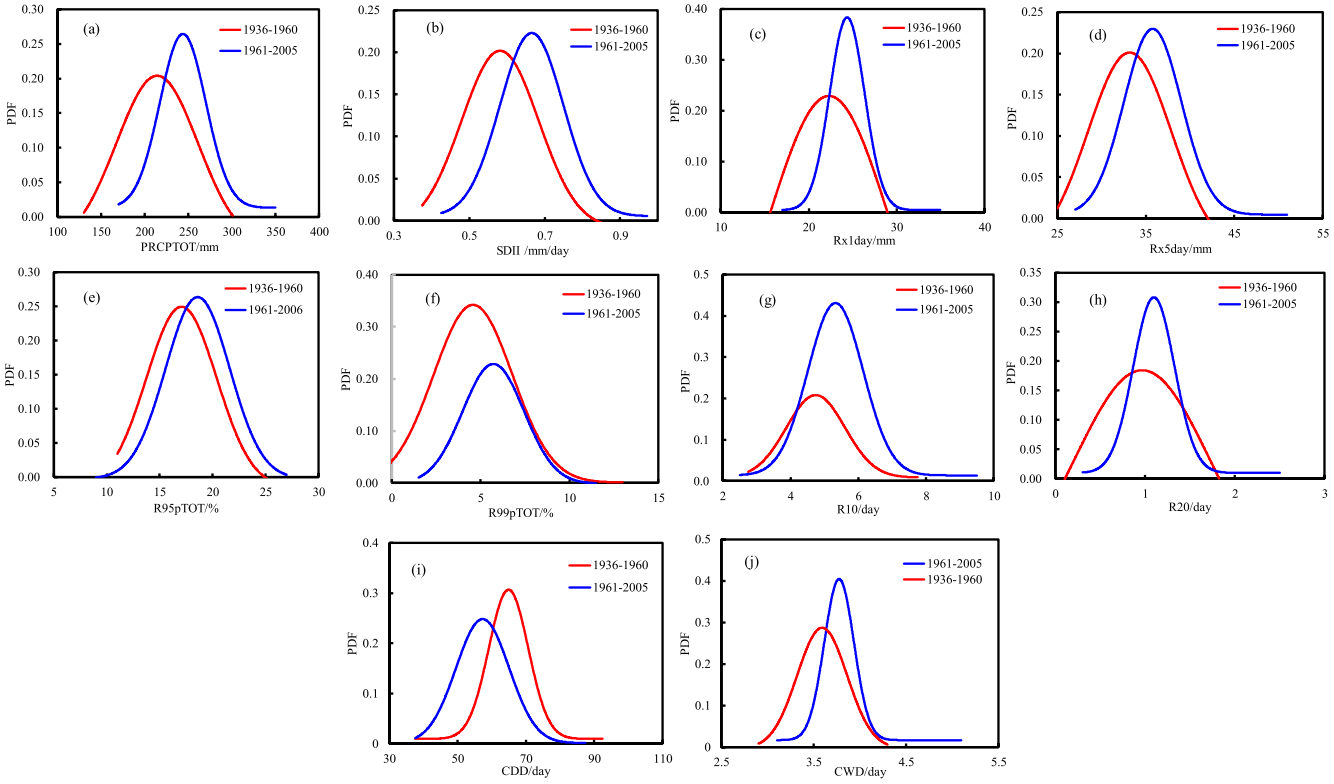

Fig. 7. Probability distribution functions of annual extreme precipitation indices (a–j) over Central Asia between 1936 and 2005 for two sub-periods: 1936–1960 (red curve) and 1961–2005 (blue curve). (For interpretation of the references to color in this figure legend, the reader is referred to the web version of this article.)

Table 3
Percentage of light, moderate, and heavy extreme precipitation during 1936–1960 and 1961–2005.

	Group	1936–1960 (%)	1961–2005 (%)
PRCPTOT	Light (<200 mm)	36.0	6.7
	Moderate (200–250 mm)	48.0	51.1
	Heavy (>250 mm)	16.0	42.2
SDII	Light (<0.5 mm/day)	24.0	0.0
	Moderate (0.5–0.7 mm/day)	64.0	60.0
	Heavy (>0.7 mm/day)	12.0	40.0
Rx5day	Light (<30 mm)	24.0	4.4
	Moderate (30–35 mm)	44.0	28.9
	Heavy (>35 mm)	32.0	66.7

decreased in the R99pTOT, implying that the frequency of the R99p and CDD decreased with time.

The PRCPTOT, SDII, and Rx5day index values was classified into three types, respectively, and the percentage of light, moderate, and heavy extreme precipitation events are listed in Table 3. For PRCPTOT, a rapid decrease in the amount of light precipitation and a concomitant increase in the amount of heavy precipitation occurred over the second time period. Similarly, the PDFs and proportions of the SDII and Rx5day indices were consistent with those of PRCPTOT, with heavy precipitation intensity and extreme precipitation events displaying an ascending trend in Central Asia from the first to the second period. In summary, both PRCPTOT and extreme precipitation displayed a long-term increasing trend in Central Asia.

3.2. Changes in extreme precipitation projected by CMIP5 models

Fig. 8 shows the temporal evolution of projected changes in the regionally averaged extreme precipitation indices (PRCPTOT, Rx1day, and CDD) over Central Asia regions under RCP 4.5 and RCP 8.5. Generally, PRCPTOT and Rx1day were projected to increase robustly in the twenty-first century, whereas decreases in CDD were projected under both emission scenario. We also estimate temporal changes of the CMIP5 ensemble mean time series for the historical period of 1936–2005, and the linear changes of CMIP5 ensemble-mean are similar to observed changes over Central Asia, but the trend rates slightly lower than observed rates.

The majority of models and the CMIP5 MME revealed significant increases in the PRCPTOT and Rx1day, the projected median increases by the end of the twenty-first century in PRCPTOT and Rx1day are 11.98% and 9.42% under RCP4.5, and 18.14% and 22.88% under RCP8.5, respectively, relative to the reference period 1986–2005 (Fig. 9). The projected increases in Rx1day (as an indicator of extreme precipitation) were larger than those for PRCPTOT, implying that increases in total precipitation are projected to be mainly due to increases in extreme precipitation intensity. A larger increase in extreme precipitation was predicted under RCP 8.5 than that under RCP 4.5.

In contrast, the projected changes in CDD (as an indicator of drought) had a larger spread than those of the PRCPTOT and Rx1day, with some models simulating a slightly increase while others simulated a significant decrease. The CDD median change is projected to be −3.28%, and−5% by the end of the twenty-first century under RCP 4.5 and RCP 8.5, respectively (Fig. 9). Moreover, differences in the projected changes (except for CDD) under RCP 4.5 and RCP 8.5 begin to emerge in the middle of the 21st century.

The SNRs of the projected change of the PRCPTOT, Rx1day and CDD were 1.64 (2.18), 1.53 (1.67), and 0.52 (0.49) under the RCP 4.5 (RCP 8.5), respectively (Fig. 10). This indicated that the PRCPTOT and Rx1day increased robustly in all models, while the CDD displayed large inter-model uncertainty.

Fig. 11 shows the PDFs of the CMIP5 MME under the two RCPs for PRCPTOT, Rx1day, and CDD indices in Central Asia for the historical simulations (1936–1960 and 1961–2005) and 21st-century projections

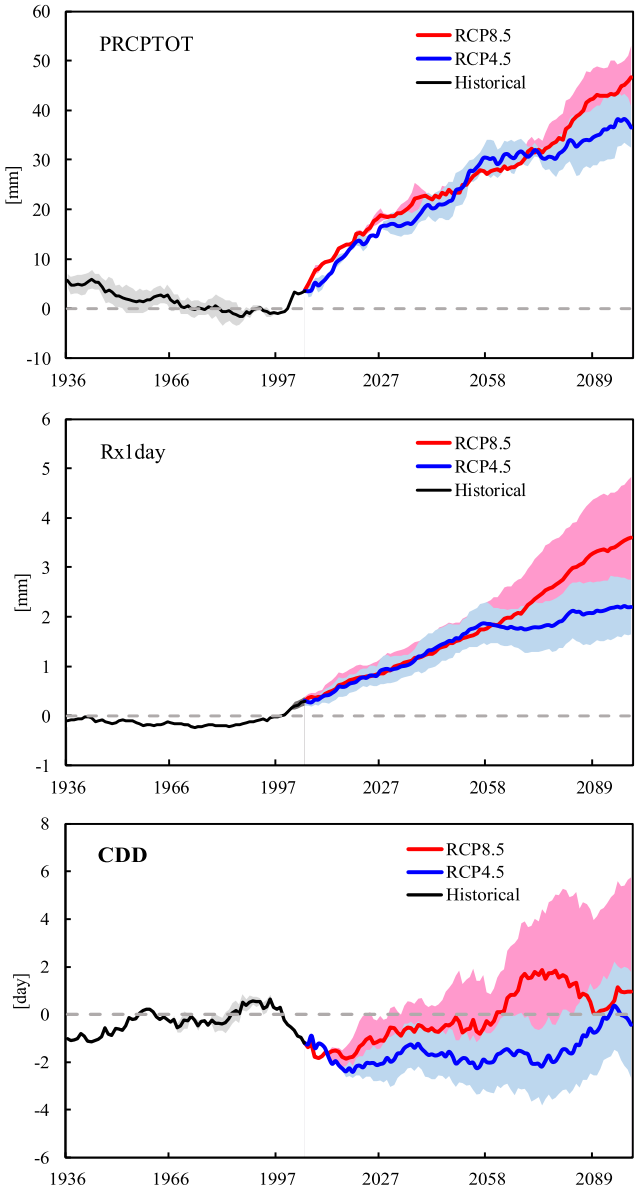

Fig. 8. Time series of anomalies of the regionally averaged extreme precipitation indices over Central Asia in the CMIP5 ensemble. Blue and red lines represent the projections from the CMIP5 multi-model ensemble for RCP 4.5 and RCP 8.5, respectively. Shading indicates the interquartile ensemble spread (25th and 75th quantiles). Black lines and gray shading indicate the results from the historical simulations. Anomaly time series are shown relative to the reference period 1986–2005 for the historical period of 1936–2005 and future simulations for 2006–2100 and were smoothed with a 21-year running mean. (For interpretation of the references to color in this figure legend, the reader is referred to the web version of this article.)

(2021–2050 and 2071–2100). For PRCPTOT, the most salient characteristic was a marked drop in the PDF peaks and concomitant shift to the right from the historical period to the 21st century (Fig. 11a and d). This suggests that PRCPTOT increased due to increases in precipitation intensity and decreases in precipitation frequency. For Rx1day, the peak location displayed a pronounced positive shift with time, and the PDF peaks reached a maximum probability during the late-21st century (Fig. 11b and e). This indicated that the intensity and frequency of extreme precipitation increased with time, especially in the late 21st century. The PDFs of CDD displayed slight positive peak shifts but were significantly raised from the historical period to the middle of the 21st century, followed by a drop in the late-21st century (Fig. 11c and f). This

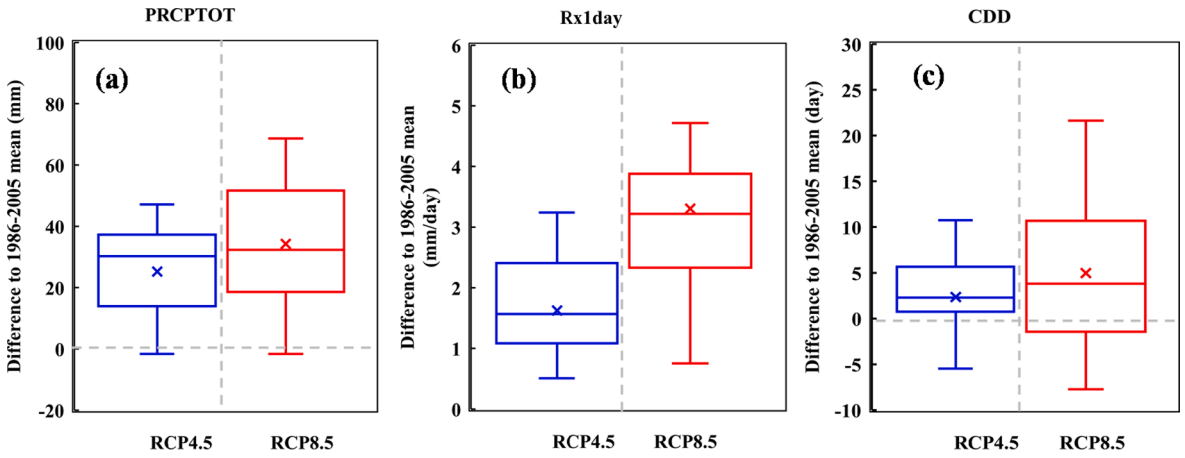

Fig. 9. Projected changes in PRCPTOT (a), Rx1day (b), and CDD (c) over the period 2071–2100 relative to the reference period 1986–2005 under RCP4.5 (blue) and RCP8.5 (red). The boxes indicate the interquartile range of the CMIP5 ensemble, whiskers indicate the 0.5–0.95 quantile range, and the cross markers represent the ensemble mean. (For interpretation of the references to color in this figure legend, the reader is referred to the web version of this article.)

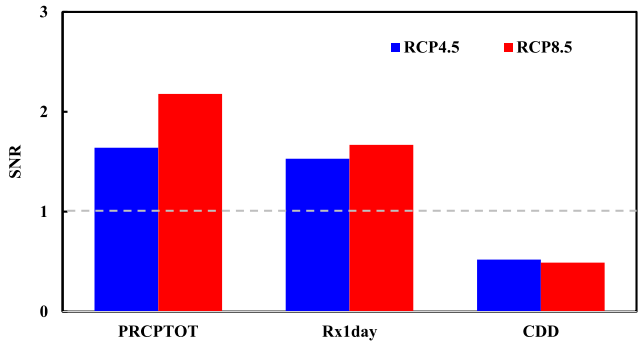

Fig. 10. The SNR of the projected change of extreme precipitation.

implied that the frequency of CDD was largest in the mid-21st century. In addition, changes in the PDFs were larger under RCP 8.5 than under RCP 4.5 for all indices and increased with time (Fig. 11).

3.3. *Response of extreme precipitation to global warming*

The responses of projected extreme precipitation in Central Asia to global warming under the two RCPs are shown in Fig. 12. The average extreme precipitation indices in Central Asia responded approximately linearly to global near-surface air temperature changes in the CMIP5 model simulations. The response rates of the PRCPTOT and Rx1day indices were larger than that of CDD, with rates of 4.95 (−3.29–13.09) %/K, 5.79 (0.95–9.68) %/K, and 2.79 (−5.95–9.36) %/K under the RCP 4.5 scenario, respectively (Fig. 12). The response rates of the Rx1day is generally consistent with (although slightly lower than) that expected from the Clausius–Clapeyron relationship. The thermodynamic arguments declare an increase rate in extreme precipitation similar to the moisture increase (7%/K), as extreme precipitation is largely driven by moisture convergence (Trenberth et al., 2003; Zhang et al., 2018). The slightly lower response of the Rx1day in simulations compared to the thermodynamic arguments indicates a potential offset from the dynamic changes overall, which can substantially affect extreme precipitation (O'Gorman and Schneider, 2009; 2015; Pfahl et al., 2017).

In addition, the response rates were slightly lower under RCP 8.5 than under RCP 4.5 for all indices (Fig. 12). Specifically, there is a positive response rates of the Rx1day under RCPs, and also shows a relatively smaller spread between different model simulations. Thus, all simulations give a positive response of Rx1day to greenhouse gas (GHG) radiative forcing, implying extreme precipitation is the most sensitive to warming. The PRCPTOT and Rx1day responses were robust against model spread with high SNRs, but the CDD displayed a moderate response with a low SNR (Fig. 12b).

4. Discussion

Central Asia is likely to be strongly impacted by global warming, resulting in increases in extreme precipitation. Here we investigate long term changes in annual precipitation totals and extremes over Central Asia using continuous observations. The total and extreme precipitation averaged over Central Asia shows robust increases during 1936–2005. Moreover, the frequency and intensity of extreme precipitation increased with time. Zhang et al. (2017) also found that all precipitation indices in Central Asia displayed an increasing trend over 1938–2005 except CDD, and abrupt changes occurred around 1957. Our analysis suggested that an abrupt change in both PRCPTOT and Rx1day occurred in 1960. Previous studies also indicated that precipitation variables experienced a marked change around the 1960s in Central Asia and Kazakhstan (Chen et al., 2011; Salnikov et al., 2015; Xu et al., 2015), consistent with the results of our study. However, larger uncertainty existed in the results of the previous studies as a consequence of the sparse observational coverage in Central Asia.

The theoretical models declare an exponentially increase in extreme precipitation intensity with temperatures at a rate, in the absence of moisture limitation (Trenberth, 1999; Trenberth et al., 2003). Some station observations and climate models suggested a distinct link between extreme precipitation and temperature (Hardwick Jones et al., 2010; Utsumi et al., 2011; Lenderink et al., 2011; Shaw et al., 2011; Mishra et al., 2012; Wang et al., 2017), with extreme precipitation increasing during warm periods and decreasing during cold periods (Allan and Soden, 2008). In this study, we also investigated the relationship between extreme precipitation and local temperature in Central Asia, and it is suggested that as temperatures increase, the extreme precipitation also will increase, especially from the 1960s. The confidence estimate is that the local temperature has increased at a rate of 0.30 °C/decade from the 1960s to the 2000s based on the continuous observations and CRU (Hu et al., 2014; Yu et al., 2020). Generally, the extreme precipitation is expected to intensify with local warming as a consequence of increased water-holding capacity of the atmosphere as determined by the Clausius-Clapeyron equation (Trenberth et al., 2003; Donat et al., 2019). In particular, the relationship between extreme precipitation and local temperature does not imply cause and effect, with higher temperature potentially being correlated with specific synoptic systems, and thus different precipitation regimes (Trenberth and Shea, 2005; Haerter and Berg, 2009; Hardwick Jones et al., 2010).

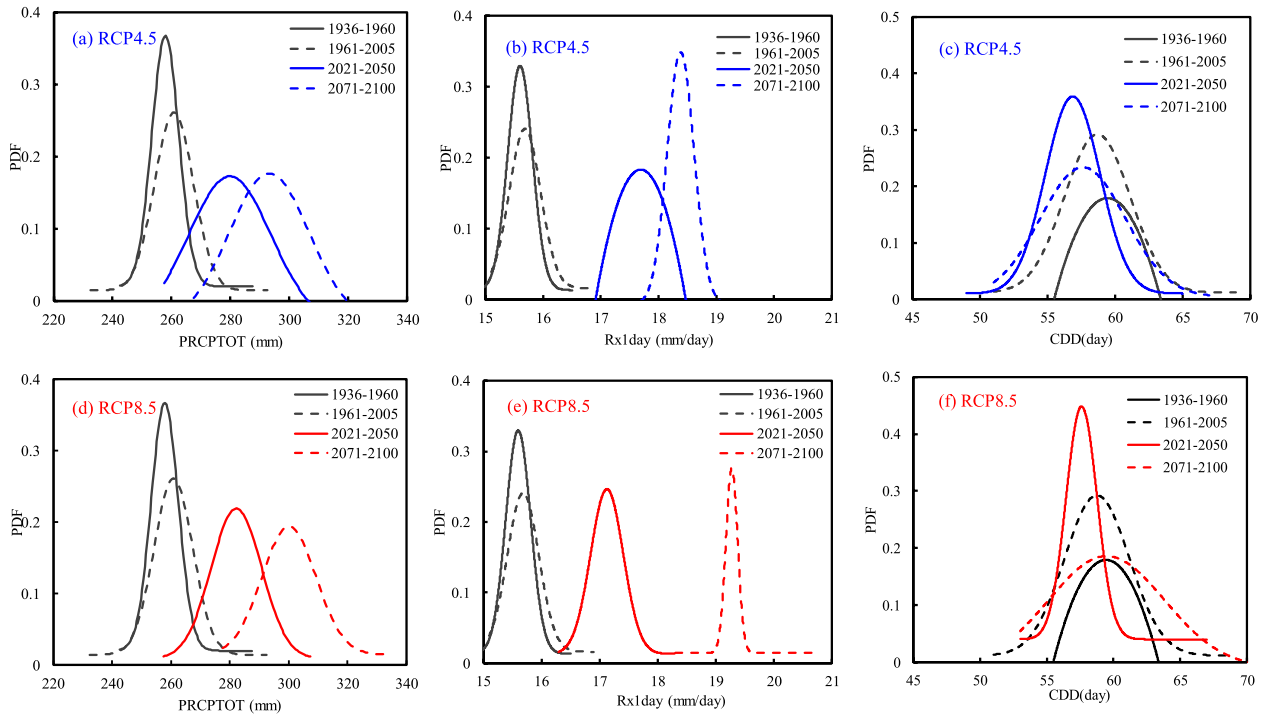

Fig. 11. Probability distribution functions of CMIP5 MME for PRCPTOT, Rx1day, and CDD in Central Asia. Four periods are shown: historical simulations of 1936–1960 and 1961–2005 and 21st-century projections for 2021–2050 and 2071–2100. The blue and red lines represent the projections from the CMIP5 MME under the RCP 4.5 and RCP 8.5 scenarios, respectively. (For interpretation of the references to color in this figure legend, the reader is referred to the web version of this article.)

Thus, the physical mechanisms of change in extreme precipitation in a warming climate need to be considered both thermodynamic arguments, and the dynamics of atmospheric circulation and moisture advection (Hardwick Jones et al., 2010).

This study confirmed the intensification of total and extreme precipitation in Central Asia based on observational records and CMIP5 model simulations. Donat et al. (2019) also predicted the intensification of extremes during the 21st century in arid regions worldwide but found no significant changes in total and extreme precipitation based on the GHCNDEX (Donat et al., 2013a) and HadEX2 (Donat et al., 2013b). Thus, the spatial patterns of extreme changes in global arid regions were heterogeneous. A consistent increase in total precipitation was identified in Central Asia, including arid areas of China and around the Tibetan Plateau (Alexander et al., 2006; You et al., 2008; Wang et al., 2013), but total and extreme precipitation in the Middle Eastern region has displayed an opposing trend (Zhang et al., 2005). This implies that extreme precipitation has increased to a greater extent in Central Asia than in other arid regions.

In Central Asia, extreme precipitation indices such as PRCPTOT, Rx1day, and CDD increased approximately linearly with global warming, at rates of 4.95%/K, 5.79%/K, and 2.79%/K under RCP 4.5. The response rates were slightly lower under RCP 8.5 than under RCP 4.5 for all indices. Previous studies also showed a statistically significant regression relationship between daily extreme precipitation increases and the magnitude of global warming (Allen and Ingram, 2002; Lambert and Webb, 2008; Donat et al., 2016). For arid regions, the PRCPTOT-temperature regression slope was about 15%/K, and the rate of increase in extreme precipitation (Rx1day) was between 6% and 7%/K

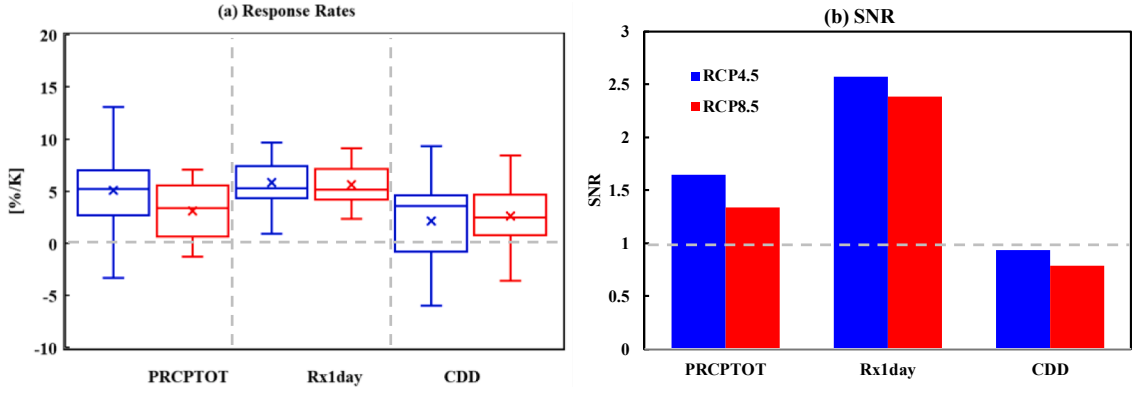

Fig. 12. Response of extreme precipitation to global warming. (a) Response rates of the extreme precipitation indices change over Central Asia to the global mean surface air temperature change in the different CMIP5 simulations under the RCP 4.5 (blue) and RCP 8.5 (red) scenarios. Boxes indicate the interquartile range of the CMIP5 ensemble, whiskers show the 0.5–0.95 quantile range, and the cross markers represent the multimodel ensemble medians. (b) The SNR of extreme precipitation responses. Signal refers to multimodel median responses, and noise refers to intermodel standard deviations. (For interpretation of the references to color in this figure legend, the reader is referred to the web version of this article.)

under both RCP 4.5 and RCP 8.5 (Donat et al., 2016). Peng et al. (2019) evaluated the response of extreme precipitation to global warming, with Rx1day, Rx5day, and SDII index response rates of 6.30%/K, 5.71%/K, and 4.99%/K, respectively, under RCP 8.5. These results are similar to those obtained in our study and close to the 6–7%/K warming range indicated by the Clausius-Clapeyron relationship (Trenberth et al., 2003).

Increasing total precipitation in Central Asia is mainly due to the intensification of extreme precipitation and a concomitant weakening of light precipitation with a simultaneous overcompensation of increased evaporation in response to global warming (Held and Soden, 2006; Roderick et al., 2014). Water availability will therefore remain limited in a warmer climate over Central Asia. Generally, the limited availability of atmospheric water in Central Asia does not promote extreme precipitation events. This suggests that extreme precipitation could be a consequence of atmospheric moisture convergence from remote moisture sources that are transported to Central Asia through large-scale atmospheric flows. Moisture is mainly transported by midlatitude westerlies as they flow from the North Atlantic and Arctic oceans (Yao et al., 2016; Huang et al., 2015). Summer precipitation in Central Asia is positively affected by sea surface temperature in the Indian Ocean or the Indian monsoon, which brings tropical moisture into Central Asia and promotes extreme precipitation (Zhao and Zhang, 2016; Huang et al., 2015, 2017). In addition, the El Niño/Southern Oscillation inevitably affects extreme precipitation and dry/wet conditions in Central Asia (Chen et al., 2018; Hu et al., 2019). We therefore suggest that extreme precipitation changes in Central Asia are not regulated by local water availability but are rather controlled by large-scale atmospheric flows.

5. Conclusions

Central Asia is likely to be strongly impacted by global warming, resulting in increases in extreme precipitation. In this study, we used extreme precipitation indices (PRCPTOT, SDII, Rx1day, Rx5day, R10, R20, R95pTOT, R99pTOT, CDD, and CWD) to investigate changes in total and extreme precipitation in Central Asia based on observational records and CMIP5 model simulations. The main conclusions can be summarized as follows.

For the regionally averaged trend in Central Asia, all of the extreme indices except for CDD, displayed an increasing trend for 1936–2005, with change rates of 9.78 mm (PRCPTOT), 0.03 mm/day (SDII), 0.45 mm/day (Rx1day), 0.79 mm (Rx5day), 0.23 days (R10), 0.06 days (R20), 0.27% (R95pTOT), 0.21% (R99pTOT), and 0.04 days (CWD) per decade; the decreasing trend for CDD was −2.02 days per decade. The trends for PRCPTOT, SDII, Rx1day, Rx5day, R10, R20, and CDD were statistically robust. Moreover, the frequency and intensity of extreme precipitation increased with time.

Based on the CMIP5 model simulations, the PRCPTOT and Rx1day were projected to increase robustly in the twenty-first century, whereas decreases in CDD were projected under RCP 4.5 and RCP 8.5. The projected increases in Rx1day were larger than those for PRCPTOT, implying that increases in total precipitation are projected to be mainly due to increases in extreme precipitation intensity. A larger increase in extreme precipitation was predicted under RCP 8.5 than that under RCP 4.5. For the PDFs of the CMIP5 MME, the PRCPTOT increased due to heightened precipitation intensity rather than a change in precipitation frequency, and both the intensity and frequency of Rx1day increased with time in the late-21st century, while the frequency of CDD was largest in the mid-21st century.

The average extreme precipitation indices in Central Asia responded approximately linearly to global near-surface air temperature changes in the CMIP5 model simulations. The response rates of the PRCPTOT and Rx1day indices were larger than that of CDD, with rates of 4.95%/K, 5.79%/K, and 2.79%/K under the RCP 4.5 scenario, respectively.

In conclusion, our results highlight the likely intensification of total and extreme precipitation in Central Asia under climatic warming. With more water availability, the increase in extreme precipitation may lead to an increased risk of flooding and impact infrastructure and oasis agricultural security. Thus, future opportunities and challenges are similar across Central Asia, additional adaptation measures are necessary to mitigate climate change-related issues.

CRediT authorship contribution statement

Junqiang Yao: Conceptualization, Writing - original draft, Methodology, Formal analysis. **Yaning Chen:** Conceptualization, Writing - review & editing, Validation. **Jing Chen:** Methodology, Software, Formal analysis. **Yong Zhao:** Software, Validation, Writing - review & editing. **Dilinuer Tuoliewubieke:** Writing - original draft, Software. **Jiangang Li:** Software, Data curation, Investigation, Formal analysis. **Lianmei Yang:** Supervision, Visualization, Software. **Weiyi Mao:** Data curation, Investigation, Validation.

Declaration of competing interest

The authors declare that they have no known competing financial interests or personal relationships that could have appeared to influence the work reported in this paper.

Acknowledgements

This work was funded by the National Key Research and Development Program of China (2018YFC1507101), National Natural Science Foundation of China (U1903208, U1903113), Sichuan Science and Technology Program (2020JDJQ0050) and Climate Change Special Project of China Meteorological Administration (CCSF202028).

Appendix A. Supplementary data

Supplementary data to this article can be found online at https://doi.org/10.1016/j.jhydrol.2020.125760.

References

Aguilar, E., et al., 2005. Changes in precipitation and temperature extremes in Central America and northern South America, 1961–2003. J. Geophys. Res. 110, D23107 https://doi.org/10.1029/2005JD006119.

Alexander, L.V., 2016. Global observed long-term changes in temperature and precipitation extremes: a review of progress and limitations in IPCC assessments and beyond. Weather Clim. Extremes 11, 4–16.

Alexander, L.V., Zhang, X., Peterson, T.C., Caesar, J., Gleason, B., Klein Tank, A.M.G., Haylock, M., Collins, D., Trewin, B., Rahimzadeh, F., Tagipour, A., Rupa Kumar, K., Revadekar, J., Griffiths, G., Vincent, L., Stephenson, D.B., Burn, J., Aguilar, E., Brunet, M., Taylor, M., New, M., Zhai, P., Rusticucci, M., Vazquez-Aguirre, J.L., 2006. Global observed changes in daily climate extremes of temperature and precipitation. J. Geophys. Res. 111, D5. https://doi.org/10.1029/2005jd006290.

Alexander, L.V., Fowler, H.J., Bador, M., Behrangi, A., Donat, M.G., Dunn, R., Seneviratne, S.I., 2019. On the use of indices to study extreme precipitation on sub-daily and daily timescales. Environmental Research Letters 14 (12), 125008.

Allan, R.P., Soden, B.J., 2008. Atmospheric warming and the amplification of precipitation extremes. Science 321 (5895), 1481–1484.

Allen, M.R., Ingram, W.J., 2002. Constraints on future changes in climate and the hydrologic cycle. Nature 419, 224–232.

Chen, F., Wang, J., Jin, L., Zhang, Q., Li, J., Chen, J., 2009. Rapid warming in mid-latitude central Asia for the past 100 years. Front. Earth Sci. China 3 (1), 42–50.

Chen, F.H., Huang, W., Jin, L.Y., Chen, J.H., Wang, J.S., 2011. Spatiotemporal precipitation variations in the arid Central Asia in the context of global warming. Sci. China Earth Sci. Chin. J. 41, 1647e1657. https://doi.org/10.1007/s11430-011-Asia 4333-8.

Chen, G., Huang, R., 2012. Excitation mechanisms of the teleconnection patterns affecting the July precipitation in Northwest China. J. Clim. 25, 7834–7851.

Chen, X., Wang, S., Hu, Z., Zhou, Q., Hu, Q., 2018. Spatiotemporal characteristics of seasonal precipitation and their relationships with ENSO in Central Asia during 1901–2013. J. Geogr. Sci. 28 (9), 1341–1368.

Dai, X.G., Wang, P., 2017. A new classification of large-scale climate regimes around the Tibetan Plateau based on seasonal circulation patterns. Adv. Clim. Chang. Res. 8, 26–36.

Deng, H.J., Chen, Y.N., Shi, X., Li, W.H., 2014. Dynamics of temperature and precipitation extremes and their spatial variation in the arid region of northwest China. Atmos. Res. 138, 346–355.

Donat, M.G., Alexander, L.V., Yang, H., Durre, I., Vose, R., Caesar, J., 2013a. Global land-based datasets for monitoring climatic extremes Bull. Am. Meteorol. Soc. 94, 997–1006.

Donat, M.G., et al., 2013b. Updated analyses of temperature and precipitation extreme indices since the beginning of the twentieth century: the HadEX2 dataset. J. Geophys. Res. Atmos. 118, 2098–2118.

Donat, M.G., Lowry, A.L., Alexander, L.V., O'Gorman, P.A., Maher, N., 2016. More extreme precipitation in the world's dry and wet regions Nat. Clim. Chang. 6, 508–513.

Donat, M.G., Angélil, O., Ukkola, A.M., 2019. Intensification of precipitation extremes in the world's humid and water-limited regions. Environ. Res. Lett. 14 (6), 065003.

Du, H., Alexander, L.V., Donat, M.G., Lippmann, T., Srivastava, A., Salinger, J., et al., 2019. Precipitation from persistent extremes is increasing in most regions and globally. Geophys. Res. Lett. 46 https://doi.org/10.1029/2019GL081898.

Feng, R., Yu, R., Zheng, H., Gan, M., 2017. Spatial and temporal variations in extreme temperature in Central Asia. Int. J. Climatol. 38, 388–400.

Frich, P., Alexander, L.V., Della-Marta, P., Gleason, B., Haylock, M., Klein Tank, A.M.G., Peterson, T., 2002. Observed coherent changes in climatic extremes during the second half of the twentieth century. Clim. Res. 19, 193–212.

Gemmer, M., Fischer, T., Jiang, T., Su, B., Liu, L.L., 2011. Trends in precipitation extremes in the Zhujiang River basin, South China. J. Clim. 24 (3), 750–761.

Guan, X., Yang, L., Zhang, Y., et al., 2019. Spatial distribution, temporal variation, and transport characteristics of atmospheric water vapor over Central Asia and the arid region of China. Glob. Planet. Chang. 159–178.

Haerter, J.O., Berg, P., 2009. Unexpected rise in extreme precipitation caused by a shift in rain type? Nat. Geosci. 2, 372–373. https://doi.org/10.1038/ngeo523.

Hardwick Jones, R., et al., 2010. Observed relationships between extreme sub-daily precipitation, surface temperature, and relative humidity. Geophys. Res. Lett. 37, L22805.

Held, I.M., Soden, B.J., 2006. Robust responses of the hydrological cycle to global warming. J. Clim. 19, 5686–5699.

Herger, N., Abramowitz, G., Knutti, R., Angélil, O., Lehmann, K., Sanderson, B.M., 2018. Selecting a climate model subset to optimise key ensemble properties. Earth Syst. Dyn. 9 (1), 135–151.

Hu, Z., Zhang, C., Hu, Q.S., Tian, H., 2014. Temperature changes in Central Asia from 1979 to 2011 based on multiple datasets. Journal of Climate 27. https://doi.org/10.1175/JCLI-D-13-00064.1.

Hu, Z., Hu, Q., Zhang, C., Chen, X., Li, Q., 2016. Evaluation of reanalysis, spatially interpolated and satellite remotely sensed precipitation data sets in central Asia. J. Geophys. Res. Atmos. 121 (10), 5648–5663.

Hu, Z., Zhou, Q., Chen, X., Qian, C., Wang, S., Li, J., 2017. Variations and changes of annual precipitation in Central Asia over the last century. International Journal of Climatology 157–170.

Hu, Z., Chen, X., Chen, D., Li, J., Wang, S., Zhou, Q., Guo, M., 2019. "Dry gets drier, wet gets wetter": A case study over the arid regions of central Asia. International Journal of Climatology 39 (2), 1072–1091.

Huang, W., Feng, S., Chen, J.-H., et al., 2015. Physical mechanisms of summer precipitation variations in the Tarim Basin in northwestern China. J. Clim. 28 (9), 3579–3591.

Huang, W., Chang, S.Q., Xie, C.L., Zhang, Z.P., 2017. Moisture sources of extreme summer precipitation events in North Xinjiang and their relationship with atmospheric circulation. Adv. Clim. Chang. Res. 8 (1), 12–17.

Intergovernmental Panel on Climate Change (IPCC), 2013. In: Stocker, T.F., et al. (Eds.), Climate Change 2013: The Physical Science Basis: Working Group I Contribution to the Fifth Assessment Report of the Intergovernmental Panel on Climate Change. Cambridge Univ Press, Cambridge, United Kingdom and New York, NY, USA.

Jiang, J., Zhou, T., Chen, X., Zhang, L., 2020. Future changes in precipitation over Central Asia based on CMIP6 projections. Environ. Res. Lett. https://doi.org/10.1088/1748-9326/ab7d03.

Kay, Art, 2012. Operational Amplifier Noise. Elsevier. https://doi.org/10.1016/C2009-0-18189-8.

Kendall, M.G., 1975. Rank-Correlation Measures. Charles Griffin, London.

Klein Tank, A.M.G., Peterson, T.C., Quadir, D.A., et al., 2006. Changes in daily temperature and precipitation extremes in central and south Asia. J. Geophys. Res. 111, D16105 https://doi.org/10.1029/2005JD006316.

Lambert, F.H., Webb, M.J., 2008. Dependency of global mean precipitation on surface temperature. Geophys. Res. Lett. 35, L16706.

Lenderink, G., et al., 2011. Scaling and trends of hourly precipitation extremes in two different climate zones—Hong Kong and the Netherlands. Hydro. Earth Syst. Sci. 15, 3033–3041.

Li, B., Chen, Y., Chen, Z., Xiong, H., Lian, L., 2016. Why does precipitation in northwest China show a significant increasing trend from 1960 to 2010? Atmos. Res. 167, 275–284.

Li Z, Fang GH, Chen YN, et al., 2020. Agricultural water demands in Central Asia under 1.5 °C and 2.0 °C global warming. Agricultural Water Management, 231 (31), 106020. doi:10.1016/j.agwat.2020.106020.

Lioubimtseva, E., Henebry, G.M., 2009. Climate and environmental change in arid Central Asia: impacts, vulnerability, and adaptations. J. Arid Environ. 73, 963–977.

Lioubimtseva, E., Cole, R., Adams, J.M., Kapustin, G., 2005. Impacts of climate and land-cover changes in arid lands of Central Asia. J. Arid Environ. 62, 285–308.

Liu, Chang, Wei, Huang, Song, Feng, Chen, J., 2018. Spatiotemporal variations of aridity in China during 1961–2015: decomposition and attribution. Science Bulletin 63 (18), 1187–1199. https://doi.org/10.1016/j.scib.2018.07.007.

Lu, B., Li, H., Wu, J., Zhang, T., Liu, J., Liu, B., Baishan, J., 2019. Impact of El Niño and Southern Oscillation on the summer precipitation over Northwest China. Atmospheric Science Letters 20 (8). https://doi.org/10.1002/asl.928.

Luo, M., Liu, T., Meng, F., Duan, Y., Bao, A., Frankl, A., De Maeyer, P., 2019. Spatiotemporal characteristics of future changes in precipitation and temperature in Central Asia. Int. J. Climatol. 39 (3), 1571–1588.

Mann, H., 1945. Nonparametric tests against trend. Econometrica 13, 245–259.

McGree, S., Herold, N., Alexander, L., Schreider, S., Kuleshov, Y., Ene, E., Ngari, A., 2019. Recent changes in mean and extreme temperature and precipitation in the Western Pacific Islands. Journal of Climate 32 (16), 4919–4941.

Menne, M.J., Durre, I., Vose, R.S., Gleason, B.E., Houston, T.G., 2012. An overview of the global historical climatology network-daily database. J. Atmos. Ocean. Technol. 29 (7), 897–910.

Mishra, V., et al., 2012. Relationship between hourly extreme precipitation and local air temperature in the United States. Geophys. Res. Lett. 39, L16403.

O'Gorman, P.A., 2015. Precipitation extremes under climate change. Curr. Clim. Change Rep. 1, 49–59 (2015).

O'Gorman, P.A., Schneider, T., 2009. The physical basis for increases in precipitation extremes in simulations of 21st-century climate change. Proc. Natl. Acad. Sci. 106 (35), 14773–14777.

Parry, M.L., Canziani, O.F., Palutikof, J.P., van der Linden, P.J., Hanson, C.E. (Eds.), 2007. Climate Change 2007: Impacts, Adaptation and Vulnerability. Cambridge University Press (976 pp.).

Pendergrass, A. G., Lehner, F., Sanderson, B. M. & Xu, Y., 2015. Does extreme precipitation intensity depend on the emissions scenario? Geophys. Res. Lett. 42, 8767–8774 (2015).

Peng, D., Zhou, T., Zhang, L., Zhang, W., Chen, X., 2019. Observationally constrained projection of the reduced intensification of extreme climate events in Central Asia from 0.5°C less global warming. Climate Dynamics 1–18.

Peterson, T.C., Manton, M.J., 2008. Monitoring changes in climate extremes: a tale of international collaboration. B. Am. Meteorol. Soc. 89, 1266–1271.

Pfahl, S., O'Gorman, P.A., Fischer, E.M., 2017. Understanding the regional pattern of projected future changes in extreme precipitation. Nat. Clim. Chang. 7, 423–427.

Roderick, M.L., Sun, F., Lim, W.H., Farquhar, G.D., 2014. A general framework for understanding the response of the water cycle to global warming over land and ocean. Hydrol. Earth Syst. Sci. 18, 1575–1589.

Salnikov, V., Turulina, G., Polyakova, S., Petrova, Y., Skakova, A., 2015. Climate change in Kazakhstan during the past 70 years. Quat. Int. 358, 77e82. https://doi.org/10.1016/j.quaint. 2014.09. 008.10.

Sen, P.K., 1968. Estimates of the regression coefficient based on Kendall's tau. J. Am. Stat. Assoc. 63, 1379–1389. https://doi.org/10.1080/01621459.1968.10480934.

Shaw, S.B., et al., 2011. The relationship between extreme hourly precipitation and surface temperature in different hydroclimatic regions of the United States. J. Hydrometeorol. 12, 319–325.

Shi, Y.F., Shen, Y.P., Li, D.L., et al., 2003. Discussion on the present climate change from warm–dry to warm–wet in Northwest China. Quat. Sci. 23, 152–164.

Shiu, C.J., Liu, S.C., Fu, C., Dai, A., Sun, Y., 2012. How much do precipitation extremes change in a warming climate? Geophys. Res. Lett. 39 (17), L17707 https://doi.org/10.1029/2012GL052762.

Sillmann, J., Kharin, V.V., Zhang, X., Zwiers, F.W., Bronaugh, D., 2013. Climate extremes indices in the CMIP5 multimodel ensemble: part 1. Model evaluation in the present climate. J. Geophys. Res. Atmos. 118 (4), 1716–1733.

Stocker, T.F., Qin, D., Plattner, G.-K., et al., 2013. Technical summary. In: Stocker, T.F., Qin, D., Plattner, G.-K., Tignor, M., Allen, S.K., Boschung, J., Nauels, A., Xia, Y., Bex, V., Midgley, P.M. (Eds.), Climate Change 2013: The Physical Science Basis. Contribution of Working Group I to the Fifth Assessment Report of the Intergovernmental Panel on Climate Change. Cambridge University Press, Cambridge, United Kingdom and New York, NY, USA.

Sugiyama, M., Shiogama, H., Emori, S., 2010. Precipitation extreme changes exceeding moisture content increases in MIROC and IPCC climate models. Proc. Natl. Acad. Sci. 107, 571–575.

Trenberth, K., 1999. Conceptual framework for changes of extremes of the hydrologic cycle with climate change. Clim. Chang. 42, 327–339.

Trenberth, K.E., Shea, D.J., 2005. Relationships between precipitation and surface temperature. Geophys. Res. Lett. 32, L14703 https://doi.org/10.1029/2005GL022760.

Trenberth, K.E., Dai, A., Rasmussen, R.M., Parsons, D.B., 2003. The changing character of precipitation. Bull. Am. Meteorol. Soc. 84, 1205–1217.

Trenberth, K.E., Fasullo, J.T., Shepherd, T.G., 2015. Attribution of climate extreme events. Nat. Clim. Chang. 5, 725–730. https://doi.org/10.1038/nclimate2657.

UNDP, 2005. Central Asia Human Development Report. UN Development Programme (246 pp.).

Utsumi, N., et al., 2011. Does higher surface temperature intensify extreme precipitation? Geophys. Res. Lett. 38, L16708.

Wang, H.J., Chen, Y.N., Chen, Z.S., 2013. Spatial distribution and temporal trends of mean precipitation and extremes in the arid region, northwest of China, during 1960–2010. Hydrol. Process. 27, 1807e1818. https://doi.org/10.1002/hyp.9339.

Wang, G., Wang, D., Trenberth, K.E., Erfanian, A., Yu, M., Bosilovich, M.G., Parr, D., 2017. The peak structure and future changes of the relationships between extreme precipitation and temperature. Nat. Clim. Chang. 7 (4), 268–274.

Wartenburger, R., Hirschi, M., Donat, M.G., et al., 2017. Changes in regional climate extremes as a function of global mean temperature: an interactive plotting framework. Geosci. Model Dev. 10 (9), 3609–3634.

Xu, L., Zhou, H., Du, L., Yao, H., Wang, H., 2015. Precipitation trends and variability from 1950 to 2000 in arid lands of Central Asia. J. Arid Land. 7, 514–526.

Yao, J., Chen, Y., 2015. Trend analysis of temperature and precipitation in the Syr Darya Basin in Central Asia. Theoretical and Applied Climatology 521–531.

Yao, J.Q., Yang, Q., Mao, W.Y., Zhao, Y., Xu, X.B., 2016. Precipitation trend–elevation relationship in arid regions of the China. Glob. Planet. Chang. 143, 1–9.

Yao, J., Zhao, Y., Chen, Y., Yu, X., Zhang, R., 2018. Multi-scale assessments of droughts: a case study in Xinjiang, China. Sci. Total Environ. 630, 444–452.

Yao, J., Chen, Y., Zhao, Y., Guan, X., Mao, W., Yang, L., 2020. Climatic and associated atmospheric water cycle changes over the Xinjiang, China. J. Hydrol. 585, 124823. https://doi.org/10.1016/j.jhydrol.2020.124823.

You, Q., Kang, S., Aguilar, E., Yan, Y., 2008. Changes in daily climate extremes in the eastern and central Tibetan Plateau during 1961–2005. J. Geophys. Res. Atmos. 113, D07101. https://doi.org/10.1029/2007jd009389.

Yu, Y., Chen, X., Disse, M., Cyffka, B., Lei, J., Zhang, H., Brieden, A., Welp, M., Abuduwaili, J., Li, Y., Zeng, F., Gui, D., Thevs, N., Ta, Z., Gao, X., Pi, Y., Yu, X., Sun, L., Yu, L., 2020. Climate change in Central Asia: Sino-German cooperative research findings. Sci. Bull. 65 (9), 689–692.

Zhang, X.B., et al., 2005. Trends in Middle East climate extreme indices from 1950 to 2003. J. Geophys. Res. Atmos. 110, D22. https://doi.org/10.1029/2005JD006181.

Zhang, X., Alexander, L., Hegerl, G.C., Jones, P., Tank, A.K., Peterson, T.C., Zwiers, F.W., 2011. Indices for monitoring changes in extremes based on daily temperature and precipitation data. Wiley Interdisciplinary Reviews: Climate Change 2 (6), 851–870.

Zhang, M., Chen, Y., Shen, Y., Li, Y., 2017. Changes of precipitation extremes in arid Central Asia. Quat. Int. 436, 16–27.

Zhang, W., Zhou, T., Zou, L., et al., 2018. Reduced exposure to extreme precipitation from 0.5 °C less warming in global land monsoon regions. Nat Commun 9, 3153. https://doi.org/10.1038/s41467-018-05633-3.

Zhao, Y., Zhang, H., 2016. Impacts of SST Warming in tropical Indian Ocean on CMIP5 model-projected summer rainfall changes over Central Asia. Clim. Dyn. 46, 3223–3238.